Polymer Chemistry

ROYAL SOCIETY OF CHEMISTRY

PAPER

View Article Online
View Journal | View Issue

Check for updates

Cite this: *Polym. Chem.*, 2025, **16**, 687

Guanidinium-based ionic porous organic polymer as a propitious material for inordinate uptake of permanganate ions from water†

P. S. Nandamol[a] and Mintu Porel *[a,b]

Metal-based oxo anions are major contributors towards freshwater contamination. Bioaccumulation and biomagnification through food chains pose threats to the sustainability of the environment. We introduced a novel guanidinium-based cationic porous organic polymer (POP) designed for the rapid and efficient removal of permanganate *via* electrostatic interaction between a cationic polymer and the anionic pollutant permanganate. The polymer had exceptionally high uptake of 9.4 g g^{-1} for permanganate ions. This is far superior than that reported in the literature. The material exhibited rapid sorption kinetics and a removal efficiency of 100%. Moreover, selectivity, pH and recyclability experiments were evaluated to confirm the practical applicability of the material. In addition, we employed two distinct strategies for the synthesis of a guanidinium-based cationic POP: solvothermal and mechanochemical. Both polymers were characterized using CPMAS ^{13}C NMR, FT-IR, powder-XRD, N_2 sorption analysis, TGA and FE-SEM. The physicochemical properties of both polymers were compared. The polymers showed 100% removal efficiency for permanganate from aqueous solution. The mechanochemical method did not involve energy consumption, long-time duration or involvement of toxic organic solvents, so the process was environmentally benign and economically viable. The solvothermal method consumed more energy and time. Hence, the mechanochemical method was found to be more efficient, cost-effective and environmentally sustainable for the fabrication of a highly efficient guanidinium-based polymeric adsorbent material for permanganate removal from aqueous solutions.

Received 21st November 2024,
Accepted 16th December 2024

DOI: 10.1039/d4py01329h

rsc.li/polymers

1. Introduction

The explosive growth in human population and consequent global demands paved the way to an era of massive industrialization, which has resulted in extensive destruction of the environment. Freshwater contamination is one of the major challenges in the 21st century.[1] Water sources become severely contaminated by the uncontrolled discharge of industrial pollutants such as heavy metal ions, organic dyes, and radioactive contaminants from textile, electroplating, leather, paper, and printing industries, and nuclear power plants.[2] Among the various contaminants, metal oxo anions adversely affect the food chain through bioaccumulation and biomagnification. Therefore, they are among the major freshwater contaminants that require immediate remediation. The US Environmental Protection Agency (EPA) has placed such oxo anions in the priority pollutant list.[3] The International Agency for Research on Cancer has included them as a group-1 carcinogenic chemicals for humans.[4,5]

Potassium permanganate is one of the most common chemical reagents. It is widely used as an oxidizing agent in laboratories and chemical industries. Being a powerful oxidizing agent, it is highly exploited in chemical manufacture, tanning, processing of paper, wood and metals, as well as oxidation of chlorinated solvents and compounds. Advanced oxidation processes employing permanganate as the oxidant have gained paramount importance for the extraction of dyes, cyanide, phenolic compounds and other heavy metal pollutants. The National Institute of Occupational Safety and Health has confirmed that permanganate is hazardous and harmful to human health.[6] Large-scale discharge of permanganate ions from industrial effluents causes bioaccumulation and biomagnification through food chains and, hence, it is considered to be a significant contributor towards freshwater contamination. Direct exposure can cause shortness of breath, irritation to skin and eyes, whereas the long-term exposure may lead to DNA damage, and disruption to the central

[a]*Department of Chemistry, Indian Institute of Technology Palakkad, Kerala 678577, India. E-mail: mintu@iitpkd.ac.in*
[b]*Environmental Sciences and Sustainable Engineering Center, Indian Institute of Technology Palakkad, Kerala 678577, India*

† Electronic supplementary information (ESI) available. See DOI: https://doi.org/10.1039/d4py01329h

nervous system.[7] Therefore, decontamination of water bodies from permanganate ions is crucial for the sustainability and wellbeing of aquatic life.

Potassium permanganate contaminates freshwater sources through its use as an oxidant in chemical and water-treatment plants. In addition, ^{99}Tc is a hazardous radionuclide from the nuclear industry with a long half-life of 2.13×10^5 years and exists primarily as a pertechnetate ion [TcO_4^-]. It is a great challenge to carry out environmental restoration of TcO_4^- contamination due to its high solubility in water and strong mobility. Considering its radioactivity and operational difficulties, permanganate [MnO_4^-] anions have been employed as nonradioactive surrogates for TcO_4^-.[8,9]

A number of physical and chemical methods, including ion exchange, adsorption, electrodialysis, nanofiltration, chemical precipitation and membrane filtration, have been employed for the removal of toxic permanganate. Among them, adsorption is one of the most favorable because it is safe, efficient and cost-effective. The development of porous adsorbent materials from inexpensive and readily available raw materials has become a research focus. Activated carbon of coconut shells, bone and corn cob[10,11] have been explored as adsorbent materials, and one concern was the high cost of production involved. Later on, cheaper materials such as the modified powder of *Nitraria retusa*, neem and sage leaves were found to be more economical.[12–17] Metallic oxides as well as nanoparticles[18–22] have also been found to be useful for removal purposes. However, the uptake performance reported for this type of material has been much lower. Thus, poor selectivity, adsorption kinetics and uptake performance have necessitated the development of new materials for the efficient capture of oxo anions from water. Later on, wide attention was drawn towards porous cationic framework materials. Porous organic polymers (POPs) are an emerging class of polymers noted for their porous nature, high chemical and thermal stability, and functional tunability. Ionic porous organic polymers have gained paramount importance as materials capable of both ion exchange and adsorption. POPs with predesigned tunable structure, porosity, diverse functionality, chemical and thermal stability have been widely studied in terms of adsorption and gas storage. Introducing ionic structures into the framework endows them with interesting properties with respect to their electrostatic nature, which further extends their application. Moreover, a combination of microporosity and extended π conjugation provides them with exciting features.[23,24] Besides, cationic POPs have been found to be highly efficient for the sequestration of toxic oxo anions from water. Samanta *et al.* developed a chemically stable ionic viologen-organic network, and adsorption performance towards permanganate was evaluated to be 297.3 mg g^{-1}.[4] Nayak *et al.* synthesized a pyridinium-functionalized POP which showed adsorption of 333 mg g^{-1} for permanganate ions.[25] Jiao *et al.* reported targeted synthesis of a novel ionic POP with exchangeable chloride and bromide ions in the framework, which showed a total removal of 514.7 mg g^{-1} for permanganate ions.[26] Sarkar *et al.* reported a bifunctional imidazolium-functionalized ionic POP which showed an exceptionally high intake of 5372 mg g^{-1} of permanganate.[27]

Motivated by such studies, we synthesized a guanidinium-based ionic POP.[28–30] The cationic charge in the framework showed better interaction with anionic pollutants, and was responsible for the high ion-exchange ability.[31] The polymer was found to be stable, insoluble in water and most organic solvents. The material exhibited exceptionally high uptake capacity of 9.4 g g^{-1} and fast sorption kinetics for the removal of permanganate ions from aqueous solution. Our POP outperformed other POPs in the literature [Table S1†]. Furthermore, two methods were employed for the synthesis: solvothermal and mechanochemical.[32] The synthesized polymers from both methods were characterized by Fourier transform infrared (FT-IR) spectroscopy, cross-polarization magic angle spinning ^{13}C NMR spectroscopy (CPMAS ^{13}C NMR), powder X-ray diffraction (pXRD), field emission scanning electron microscopy (FE-SEM), N_2 sorption analysis and thermogravimetric analysis (TGA). A "green" mechanochemical method was found to be as efficient as a solvothermal method, and exhibited similar uptake capacity, as well as structural and physicochemical properties. The removal efficiency, kinetic studies and maximum uptake for permanganate removal were estimated further.[33–42]

2. Results and discussion

2.1. Synthesis and characterization of guanidinium-based ionic POP

A guanidinium-based ionic POP was synthesized by an imine condensation reaction between triaminoguanidinium hydrochloride [**TGDM**] and 4,4′,4″ [1,3,5-triazine-2,4,6-triyltris(oxy) tris]3-methoxybenzaldehyde [**TMB**]. The monomer **TGDM** [Scheme 1a] was synthesized by reacting guanidinium hydrochloride and hydrazine hydrate using 1,4-dioxane as the solvent under reflux condition for 2 h. The obtained solid product was collected by filtration, washed with 1,4-dioxane and dried. The product was characterized by ^{1}H NMR [Fig. S1†] and FT-IR [Fig. 1a and Fig. S2†] spectroscopy. All the proton signals of the product were confirmed in the ^{1}H NMR spectrum [Fig. S1†]. The FT-IR spectra of **TGDM** showed characteristic vibrational bands around 3350 and 3180 cm^{-1} corresponding to NH_2 stretching, and vibrational bands around 1690 cm^{-1} corresponding to imine stretching [Fig. 1a and Fig. S2†]. The monomer **TMB** [Scheme 1b] was synthesized by reacting cyanuric chloride [2.5 mmol] and vanillin [7.5 mmol] using sodium hydroxide as the base and acetone/water as the solvent. The reaction was carried out at 0 to 5 °C for 6 h. The resultant product was collected through filtration, washed with distilled water and dried. The product was characterized by ^{1}H NMR [Fig. S3†] and FT-IR [Fig. 1a and Fig. S4†] spectroscopy. The ^{1}H NMR spectrum confirmed all the proton peaks associated with the product [Fig. S3†]. The FT-IR spectra of the compound showed a carbonyl stretching band at 1700 cm^{-1}. The vibrational band around 1570 cm^{-1} corresponded to the triazine ring. The characteristic stretching

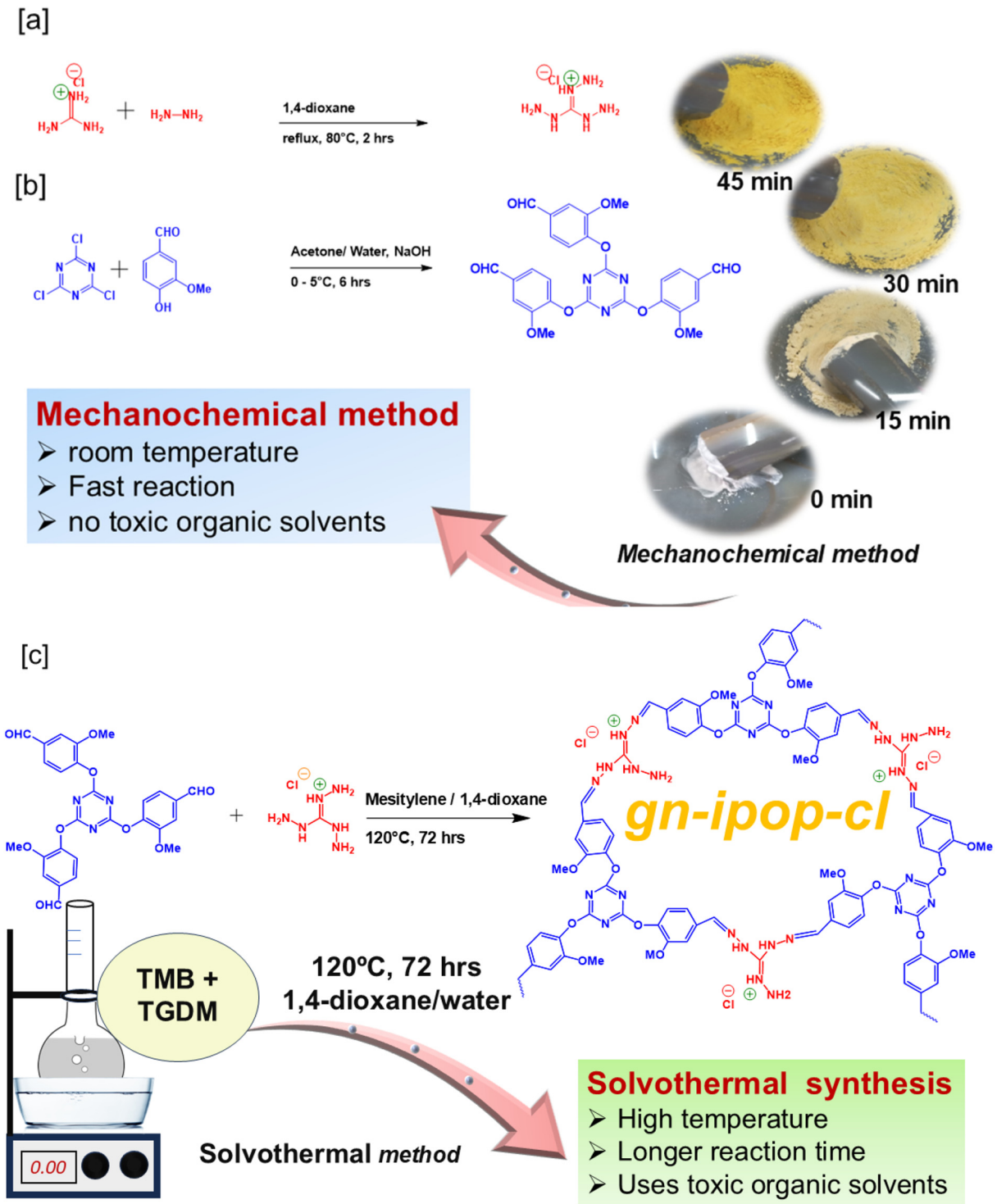

Scheme 1 Synthetic scheme for [a] **TGDM**, [b] **TMB** and [c] guanidinium-based ionic porous organic polymer **gn-ipop-cl**.

vibration of C–O was observed around 1145 cm^{-1}. The absence of hydroxyl stretching and C–Cl stretching confirmed complete conversion of the starting materials. The guanidinium-based ionic POP [**gn-ipop-cl**] was synthesized in the form of a yellow powder through a Schiff base condensation reaction between **TMB** and **TGDM**. Two distinct synthetic methodologies were explored: solvothermal and mechanochemical [Fig. S5†]. In the solvothermal method, an equimolar mixture of **TMB** and **TGDM** were taken in a Schlenk tube along with 8 mL of solvent [water and 1,4-dioxane in a ratio of 1 : 3]. The mixture was then sonicated for 1 h to disperse the monomers completely, followed by the addition of 0.2 mL of 6 M acetic acid (which served as the catalyst for the polymerization). The reaction mixture was then heated at 120 °C for 3 days. The result-

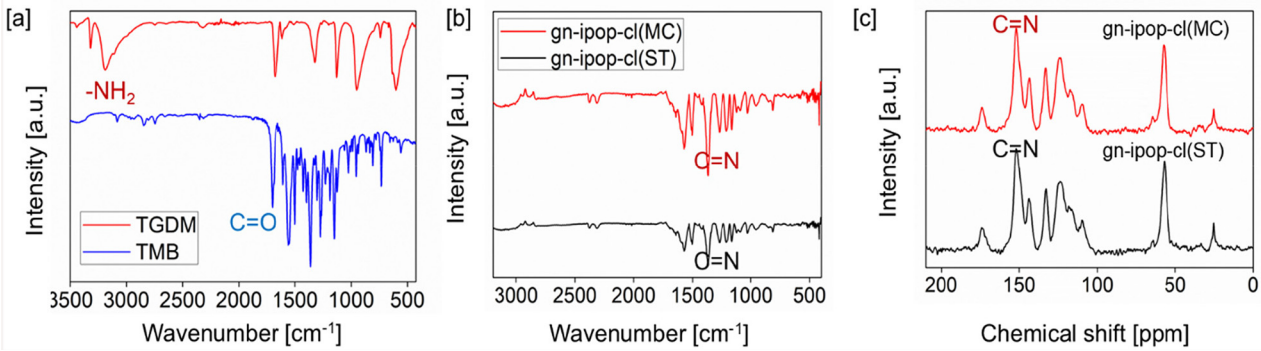

Fig. 1 [a] FT-IR spectra for **TGDM**, and **TMB**. [b] FT-IR spectra for **gn-ipop-cl**. [c] CPMAS ^{13}C NMR spectra of **gn-ipop-cl**.

ing yellow powder was filtered and washed multiple times using water, 1,4-dioxane, and acetone, and dried in an air oven overnight. The mechanochemical (or "beating and heating") method is a relatively simple, efficient, fast and feasible method for the synthesis of POPs because it follows a green synthetic pathway that does not require harsh experimental conditions, high energy consumption or the use of toxic organic solvents. Motivated by this knowledge, we employed a mechanochemical method for the synthesis of **gn-ipop-cl** and, interestingly, it was found to be more efficient than the solvothermal method. In this method, first an equimolar mixture of **TMB** and **TGDM** was taken. Then, the dry powder was slightly heated, 0.2 mL of 6 M acetic acid catalyst was added and uniformly ground for ~1 h to complete the polymerization. The collected yellow powder was then subjected to multiple washings to ensure the removal of unreacted monomeric units (if present). Both polymers were purified by Soxhlet extraction to ensure the removal of unreacted residues.

The mechanochemical synthesis was found to be advantageous in several aspects: saving time [the polymerization was completed in 45 min whereas it took 72 h for the solvothermal process], lower energy consumption, no harsh experimental conditions and, more importantly, the synthesis was devoid of toxic organic solvents. The FT-IR spectra of **TGDM** showed the characteristic vibration of the amine group around 3200 cm^{-1} [Fig. 1a]. **TMB** showed strong carbonyl stretching around 1700 cm^{-1} [Fig. 1a]. The strong absorption at 1500–1400 cm^{-1} for **gn-ipop-cl** [Fig. 1b] suggested the formation of an imine linkage through Schiff base condensation. The absence of carbonyl and amine peaks in the spectra of **gn-ipop-cl** further confirmed complete conversion of the monomers. The solid-state ^{13}C NMR spectra of **gn-ipop-cl** also confirmed the formation of an imine linkage [Fig. 1c]. The peaks observed around 140–150 ppm corresponded to imine carbon.

The powder X-ray diffraction pattern of **gn-ipop-cl(MC)** ["MC" denoting "mechanochemically synthesized polymer"] exhibited several intense peaks at 2θ 20 to 40, indicating the crystallinity of the sample. This observation could be attributed to molecular confinement in the crystal lattice of the monomer, offering precise control over the packing and crystallinity of the polymer. This effect occurred under the stimuli of heat and pressure. **gn-ipop-cl(ST)** ["ST" denoting "solvothermally synthesized polymer"] showed a broad diffraction peak suggestive of the amorphous nature of the polymer [Fig. 2a and b]. The thermal stability of the sample was analyzed using TGA, and found to be stable up to 300 °C [Fig. 2c and d].

Nitrogen-sorption analyses performed at 77 K indicated a Brunauer–Emmett–Teller (BET) surface area of 28 m^2 g^{-1} and 34 m^2 g^{-1} for **gn-ipop-cl(ST)** and **gn-ipop-cl(MC)**, respectively [Fig. 2e and f]. The pore volume obtained was 26 and 33 cc g^{-1} for gn-ipop-cl(ST) and gn-ipop-cl(MC), respectively. These values were nearly identical for the mechanochemical method as well as the solvothermal method. Furthermore, the morphological characterization of the polymer was performed using field-emission scanning electron microscopy (FE-SEM). Results indicated that the synthetic method had a great influence on the morphology of the polymer because the solvothermal and mechanochemical synthesis resulted in entirely different morphologies of the material [Fig. 3]. Elemental analyses of **gn-ipop-cl** [Fig. S6†] showed the presence of 50–60% C, 15–20% N, 25–35% O and 6–8% Cl atoms in the framework. The chemical robustness of **gn-ipop-cl(ST)** and **gn-ipop(MC)** was evaluated by incubating the material in acidic condition (2 N HCl) and basic condition (2 N NaOH) for 7 days. The structural integrity was evident from the unchanged FTIR spectra before and after treatment (Fig. S7†). The crystallinity of the polymer created by the mechanochemical method remained intact after incubation according to the pXRD pattern (Fig. S8†). The superior quality with respect to the crystallinity and environmentally benign nature of the synthesis prompted selection of **gn-ipop-cl(MC)** as an adsorbent material, and was further explored for studies on permanganate adsorption.

2.2. Studies on permanganate uptake

We constructed a guanidinium-based POP for adsorptive removal of permanganate ions because the cationic charge in the framework attracts the anionic pollutant several fold compared with a neutral molecule, and could increase the adsorption capacity. Moreover, the ionic nature of the adsorbent aids easy dispersibility in water. A biocompatible guanidinium moiety can enhance its applicability in treating real water

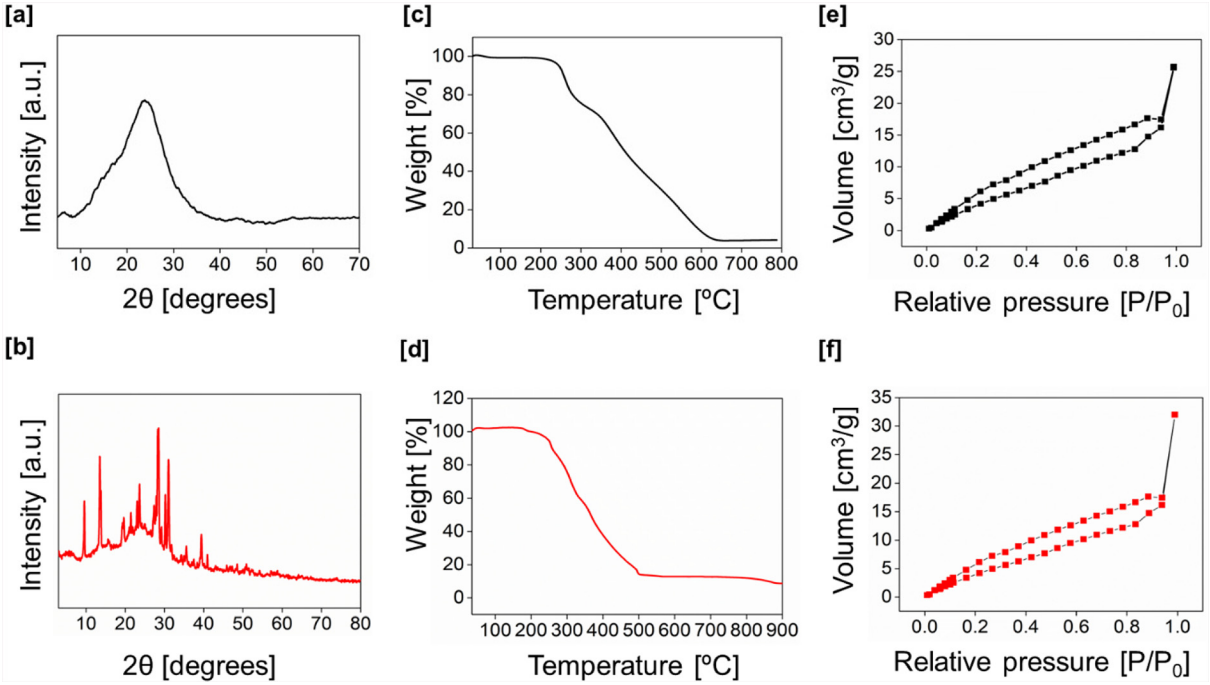

Fig. 2 pXRD pattern of [a] **gn-ipop-cl(ST)** and [b] **gn-ipop-cl(MC)**. TGA profile of [c] **gn-ipop-cl(ST)** and [d] **gn-ipop-cl(MC)**. BET surface area for [e] **gn-ipop-cl(ST)** and [f] **gn-ipop-cl(MC)**.

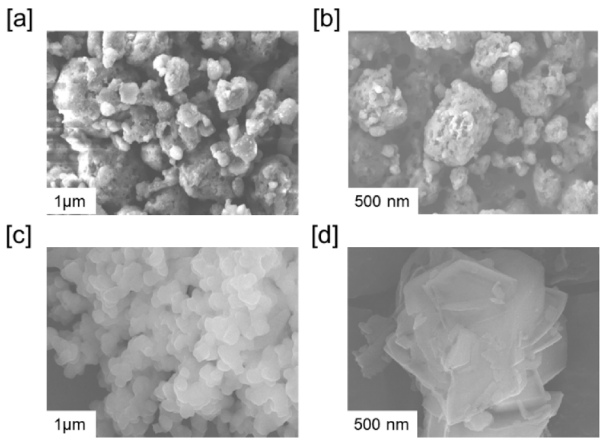

Fig. 3 Field emission scanning electron microscopy images of [a and b] **gn-ipop-cl(ST)** and [c and d] **gn-ipop-cl(MC)**.

samples. The adsorption of permanganate ions from aqueous solution by **gn-ipop-cl** was monitored by UV–Vis spectroscopy. A time-dependent study of removal of oxo anions was performed. First, a 2.5 mM aqueous solution of potassium permanganate (1 mL) was magnetically stirred along with a polymer adsorbent (1 mg). Smaller aliquots from the solution were withdrawn at regular intervals and UV–Vis spectra were recorded. The UV–Vis spectra of each solution were recorded after 10-times dilution of the original aliquots.

The decrease in absorbance of permanganate with time [Fig. 4a] clearly indicated the removal of permanganate ions from water. The polymer showed a adsorption kinetics with a removal efficiency of 100%. It was evident from the absorbance spectra that the absorbance decreased to zero after 20 min of contact for **gn-ipop-cl(MC)** and 30 min for **gn-ipop-cl(ST)** [Fig. 4c and d]. Each experiment was done in triplicate, and the final kinetic data fitted with a pseudo first-order equation and second-order rate equation. For **gn-ipop-cl(ST)** as well as **gn-ipop-cl(MC)**, kinetic data fitted well with pseudo second-order kinetics with a high R^2 value (>0.99) [Fig. 4e and f]. This finding revealed the dependence of adsorption on the concentration of permanganate as well as the number of available active sites.

In order to calculate the total uptake capacity of the polymers, 1 mg of polymer was treated with a 1 mL solution of varying concentrations of potassium permanganate. The maximum uptake capacity was calculated to be 9.397 and 9.277 g g^{-1} for **gn-ipop-cl(MC)** and **gn-ipop-cl(ST)**, respectively [Fig. 5a and b]. Data were evaluated using the Langmuir adsorption model [Fig. 5c and d]. In order to mimic the true situation, selectivity studies were performed in the presence of other competing anions [Fig. 6a and b]. Anions such as Cl^-, Br^-, NO_3^-, and SO_4^{2-} were chosen as competing anions because they are omnipresent in common water sources. An aqueous solution of targeted oxo anion and competing anion in an equimolar ratio was stirred with polymer adsorbent until equilibration, and total uptake of permanganate was evaluated. Studies on this binary mixture revealed that the removal efficiency of permanganate ions remained almost unchanged even in the presence of competing anions in the solution. Moreover, the reusability of the polymer was evaluated for up to five cycles [Fig. 6c and d]. After each cycle, the polymer was

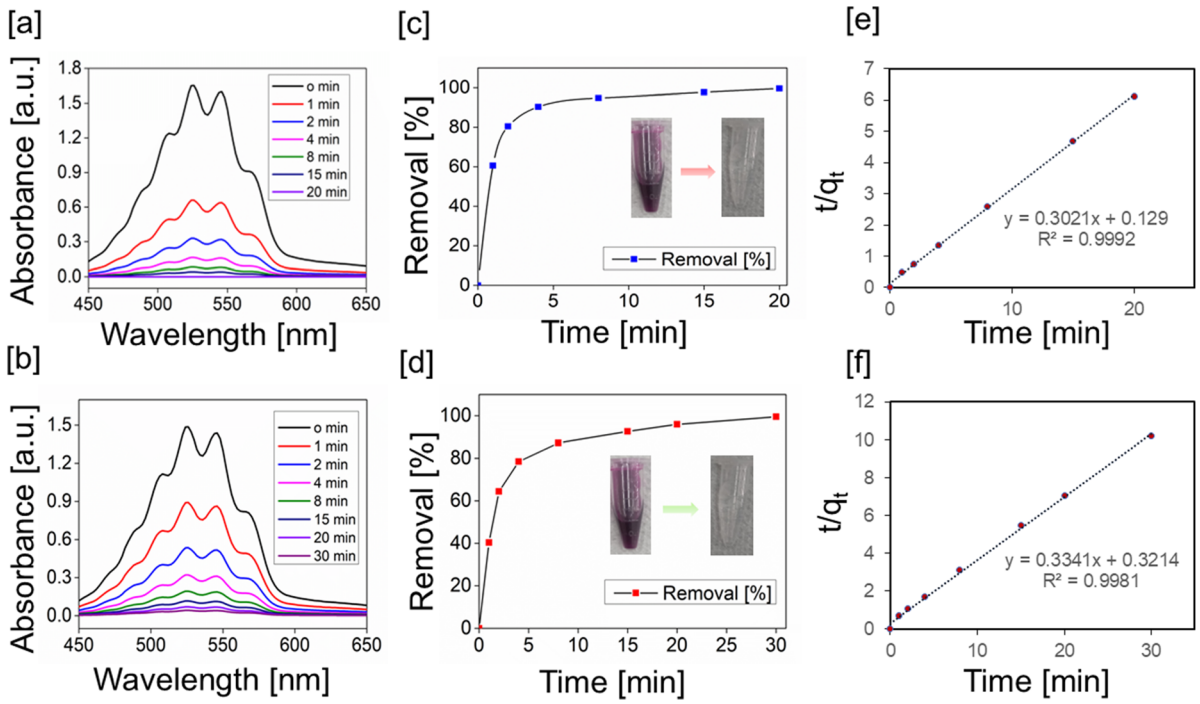

Fig. 4 UV–Vis spectra of $KMnO_4$ demonstrating the rapid uptake of permanganate in the presence of [a] **gn-ipop-cl(MC)** and [b] **gn-ipop-cl(ST)**. Plot of time *vs.* % removal of [c] **gn-ipop-cl(MC)** and [d] **gn-ipop-cl(ST)**. Second-order fitting for $KMnO_4$ adsorption for [e] **gn-ipop-cl(MC)** and [f] **gn-ipop-cl(ST)**.

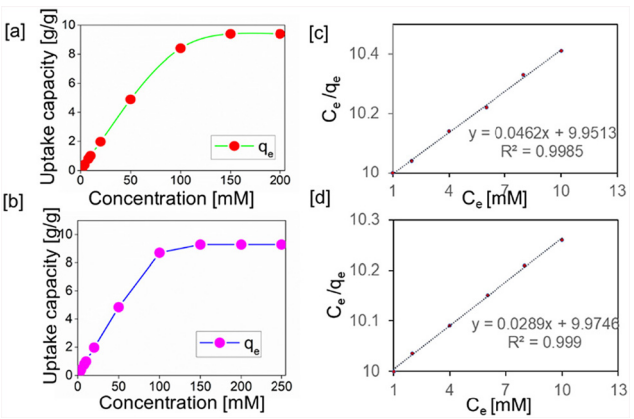

Fig. 5 Isotherm analyses of [a] **gn-ipop-cl(MC)** and [b] **gn-ipop-cl(ST)**. Langmuir adsorption model for [c] **gn-ipop-cl(MC)** and [d] **gn-ipop-cl (ST)**.

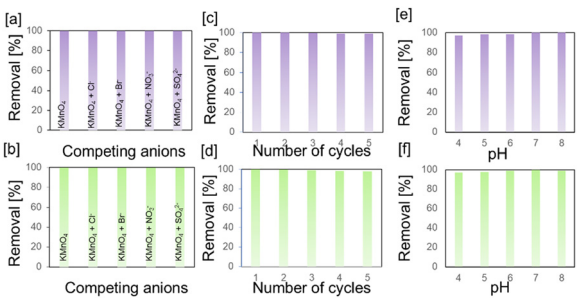

Fig. 6 Selectivity studies for [a] **gn-ipop-cl(MC)** and [b] **gn-ipop-cl(ST)**. Recyclability tests for [c] **gn-ipop-cl(MC)** and [d] **gn-ipop-cl(ST)**. pH studies for [e] **gn-ipop-cl(MC)** and [f] **gn-ipop-cl(ST)**.

collected through centrifugation, and washed with deionized water and organic solvents. It was then incubated with a saturated KCl solution for 1 day, washed and dried and used for the next cycle. The adsorption performance was also evaluated with solutions of different pH [Fig. 6e and f]. The effect of pH on removal efficiency was negligible, indicating the applicability of the material in a broad range of pH. The temperature dependence of adsorption of permanganate over **gn-ipop-cl** was also evaluated [Fig. S11†]. There was a slight decrease in the adsorption performance upon increasing the temperature from 25° to 45 °C [Fig. S11†]. This observation could be attributed to the physical nature of adsorption. The decrease in adsorption capacity with increasing temperature indicated that adsorption was exothermic in nature. This might have been due to the weakening of adsorptive forces between permanganate and the active sites on the adsorbent surface as a result of increase in temperature.

The structural integrity of post-treated materials was analyzed using FT-IR, pXRD, FE-SEM as well as EDX analyses. A vibrational stretching frequency around 1000 cm^{-1} confirmed the presence of MnO_4^- in the framework [Fig. S12†]. The crystallinity and morphology of the polymer remained unchanged after adsorption [Fig. S13 and S14†]. Elemental analyses confirmed the presence of Mn in the framework [Fig. S15†].

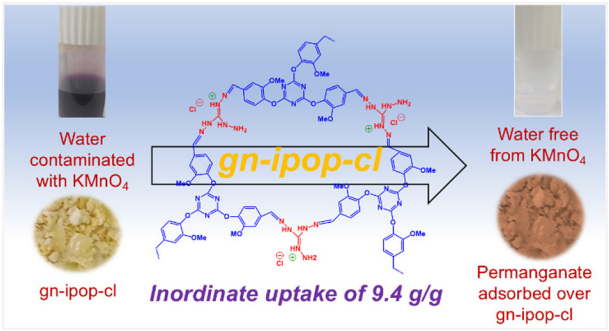

Fig. 7 Photographs of permanganate solution and polymer adsorbent before and after adsorption of permanganate.

Moreover, the negligible amount of Cl^- in the post-treated polymer suggested the possibility of ion exchange.

Thus, the material exhibited exceptionally high uptake for permanganate ions from water (Fig. 7). This finding could be attributed to the strong adsorptive interaction due to electrostatic forces between the anionic pollutant and cationic active sites in the polymer framework.

gn-ipop-cl(MC) and **gn-ipop-cl(ST)** showed identical activity in studies for the removal of permanganate ions. The mechanochemically synthesized guanidinium-based ionic POP was easier to synthesize, had a faster process and showed superior properties compared with its solvothermal analogue, and retained similar activity.

3. Conclusions

We synthesized a guanidinium-based ionic POP through the condensation of **TMB** and **TGDM** monomers following mechanochemical and solvothermal methods. Both polymers were characterized using CPMAS ^{13}C NMR, FT-IR, powder-XRD, N_2 sorption analysis, TGA and FE-SEM. The structural and physicochemical characteristics of both polymers were compared. The mechanochemical method was found to be efficient, fast, economically viable and environmentally benign. The polymer was employed for the rapid removal of permanganate ions from an aqueous solution. The polymer showed fast sorption kinetics (complete removal of permanganate ions within 20 min) and exceptionally high uptake capacity of 9.4 g g^{-1}, which is much higher than that reported in the literature (maximum uptake of 5.3 g g^{-1}). Thus, our method paves the way for the development of new, highly efficient materials based on ionic POPs for the removal of toxic oxo anions from aqueous solutions.

Author contributions

M. P. conceptualized the design of the guanidinium-based ionic POP. N. P. S. and M. P. designed the synthetic schemes. N. P. S. carried out all the syntheses, characterizations and study on permanganate removal. N. P. S. and M. P. wrote the manuscript. All authors have approved the final version of the manuscript.

Data availability

The data supporting the conclusions reached in our study have been included as part of the ESI.†

Conflicts of interest

There are no conflicts of interest to declare.

Acknowledgements

This research was funded by the Indian Institute of Technology, Palakkad, India; the Ramanujan Fellowship (SB/S2/RJN-145/2017), Science and Engineering Research Board, Department of Science and Technology, India; the Core Research Grant (CRG/2019/002495), Science and Engineering Research Board, Department of Science and Technology, India; and the Scheme for Transformational and Advanced Research in Sciences (MoE/STARS-1/293), Ministry of Education, India.

We sincerely acknowledge the Central Instrumentation Facility (CIF) at the Indian Institute of Technology, Palakkad, and SAIF Indian Institute of Science, Bangalore, India.

References

1 H. Bouwer, Integrated water management for the 21st century: problems and solutions, *J. Irrig. Drain. Eng.*, 2002, **128**(4), 193–202.
2 R. P. Schwarzenbach, T. Egli, T. B. Hofstetter, U. Von Gunten and B. Wehrli, Global water pollution and human health, *Annu. Rev. Environ. Resour.*, 2010, **35**(1), 109–136.
3 L. H. Keith and W. A. Telliard, Priority Pollutants: I. A Perspective View, *Environ. Sci. Technol.*, 1979, **13**, 416–423.
4 P. Samanta, P. Chandra, S. Dutta, A. V. Desai and S. K. Ghosh, Chemically stable ionic viologen-organic network: an efficient scavenger of toxic oxo-anions from water, *Chem. Sci.*, 2018, **9**(40), 7874–7881.
5 E. O. Oseghe, A. O. Idris, U. Feleni, B. B. Mamba and T. A. M. Msagati, A review on water treatment technologies for the management of oxoanions: prospects and challenges, *Environ. Sci. Pollut. Res.*, 2021, **28**(44), 61979–61997.
6 B. K. Marvin, J. D. Byrant, D. Root and S. Miller, Environmental health and safety issues associated with *in situ* chemical oxidation technologies, in *Proceedings of the Third International Conference on Remediation of Chlorinated and Recalcitrant Compounds*, Monterey, CA., 2002, May.

7 C. C. Willhite, V. S. Bhat, G. L. Ball and C. J. McLellan, Emergency Do Not Consume/Do Not Use concentrations for potassium permanganate in drinking water, *Hum. Exp. Toxicol.*, 2013, **32**(3), 275–298.
8 D. Banerjee, D. Kim, M. J. Schweiger, A. A. Kruger and P. K. Thallapally, Removal of TcO 4− ions from solution: materials and future outlook, *Chem. Soc. Rev.*, 2016, **45**(10), 2724–2739.
9 M. S. Lee, W. Um, G. Wang, A. A. Kruger, W. W. Lukens, R. Rousseau and V. A. Glezakou, Impeding 99Tc (IV) mobility in novel waste forms, *Nat. Commun.*, 2016, **7**(1), 12067.
10 R. K. Verma, R. Kapoor, S. K. Gupta and R. R. Chaudhari, An efficient technique for removal of K+ and MnO4− ions through adsorption in aqueous solution by using activated charcoal, *Pharm. Chem. J.*, 2014, **1**, 20–25.
11 D. J. Ezeugo and C. V. Anadebe, Removal of potassium permanganate from aqueous solution by adsorption onto activated carbon prepared from animal bone and corn cob, *Equat. J. Eng.*, 2018, 21.
12 N. A. Alamrani, H. A. Al-Aoh, M. M. Aljohani, S. A. Bani-Atta, M. Sobhi, M. Syed Khalid, A. A. A. Darwish, A. A. Keshk and M. A. Abdelfattah, Wastewater purification from permanganate ions by sorption on the Ocimum basilicum leaves powder modified by zinc chloride, *J. Chem.*, 2021, **1**, 5561829.
13 S. A. Bani-Atta, Potassium permanganate dye removal from synthetic wastewater using a novel, low-cost adsorbent, modified from the powder of Foeniculum vulgare seeds, *Sci. Rep.*, 2022, **12**(1), 4547.
14 S. A. Bani-Atta, Zinc chloride modification of sage leaves powder and its application as an adsorbent for KMnO4 removal from aqueous solutions, *Mater. Res. Express*, 2020, **7**(9), 095511.
15 H. A. Al-Aoh, Adsorption of MnO4− from aqueous solution by Nitraria retusa leaves powder; kinetic, equilibrium and thermodynamic studies, *Mater. Res. Express*, 2019, **6**(11), 115102.
16 H. A. Al-Aoh and N. A. Alamrani, Chemically modified Teucrium polium (Lamiaceae) plant act as an effective adsorbent tool for potassium permanganate (KMnO4) in wastewater remediation, *Open Chem.*, 2022, **20**(1), 736–747.
17 H. A. Al-Aoh, Equilibrium, thermodynamic and kinetic study for potassium permanganate adsorption by Neem leaves powder, *Desalin. Water Treat.*, 2019, **170**, 101–110.
18 M. Rashad, Performance efficiency and kinetic studies of water purification using ZnO and MgO nanoparticles for potassium permanganate, *Opt. Quantum Electron.*, 2019, **51**, 1–13.
19 M. M. Aljohani and H. A. Al-Aoh, Adsorptive removal of permanganate anions from synthetic wastewater using copper sulfide nanoparticles, *Mater. Res. Express*, 2021, **8**(3), 035012.
20 M. E. Mahmoud, A. A. Yakout, S. R. Saad and M. M. Osman, Removal of potassium permanganate from water by modified carbonaceous materials, *Desalin. Water Treat.*, 2016, **57**(33), 15559–15569.
21 M. Rashad, S. A. Al-Ghamdi, A. O. M. Alzahrani, K. Al-Tabaa, S. Al-Osemi, O. Al-Atawi, N. Al-Anzi, S. A. Issa and A. M. Abd-Elnaiem, Zinc oxide nanoparticles for adsorption of potassium permanganate from wastewater using shaking method, *Desalin. Water Treat.*, 2021, (229), 227–234.
22 F. Keyvani, S. Rahpeima and V. Javanbakht, Synthesis of EDTA-modified magnetic activated carbon nanocomposite for removal of permanganate from aqueous solutions, *Solid State Sci.*, 2018, **83**, 31–42.
23 Y. Byun, S. H. Je, S. N. Talapaneni and A. Coskun, Advances in porous organic polymers for efficient water capture, *Chem. – Eur. J.*, 2019, **25**(44), 10262–10283.
24 Q. Sun, B. Aguila, Y. Song and S. Ma, Tailored porous organic polymers for task-specific water purification, *Acc. Chem. Res.*, 2020, **53**(4), 812–821.
25 S. Nayak, A. Sahoo, G. S. Naidu, A. Giri and A. Patra, Pyridinium–Functionalized Ionic Porous Organic Polymer for Rapid Scavenging of Oxoanions from Water, *Macromol. Rapid Commun.*, 2023, **44**(15), 2300138.
26 S. Jiao, L. Deng, X. Zhang, Y. Zhang, K. Liu, S. Li, L. Wang and D. Ma, Evaluation of an ionic porous organic polymer for water remediation, *ACS Appl. Mater. Interfaces*, 2021, **13**(33), 39404–39413.
27 S. Sarkar, A. Chakraborty, R. Ranjan, P. Nag, S. R. Vennapusa and S. Mukhopadhyay, A bifunctional imidazolium-functionalized ionic porous organic polymer in water remediation, *Mater. Chem. Front.*, 2022, **6,(20)**, 3070–3083.
28 Z. Zhang, X. Dong, J. Yin, Z. G. Li, X. Li, D. Zhang, T. Pan, Q. Lei, X. Liu, Y. Xie and F. Shui, Chemically stable guanidinium covalent organic framework for the efficient capture of low-concentration iodine at high temperatures, *J. Am. Chem. Soc.*, 2022, **144**(15), 6821–6829.
29 S. S. Qin, Z. K. Wang, L. Hu, X. H. Du, Z. Wu, M. Strømme, Q. F. Zhang and C. Xu, Dual-functional ionic porous organic framework for palladium scavenging and heterogeneous catalysis, *Nanoscale*, 2021, **13**(7), 3967–3973.
30 P. Zhao, X. Zhou, Y. Huang, Y. Xu, S. Chen, C. Zheng, Y. Jin and C. Xia, Cationic covalent organic polymers based on guanidine with higher positive potential for selective sorption of ReO4−: Synthesis and DFT calculation, *Surf. Interfaces*, 2022, **29**, 101788.
31 H. Luo, G. S. H. Poon Ho, C. Li, J. Huang, Z. L. Xu and Y. Kim, Ionic Porous Organic Polymers Synthesized Using Solvothermal and Mechanochemical Methods as Solid Electrolytes for Lithium Metal Batteries, *Ind. Eng. Chem. Res.*, 2023, **62**(39), 15790–15797.
32 N. Brown, Z. Alsudairy, R. Behera, F. Akram, K. Chen, K. Smith-Petty, B. Motley, S. Williams, W. Huang, C. Ingram and X. Li, Green mechanochemical synthesis of imine-linked covalent organic frameworks for high iodine capture, *Green Chem.*, 2023, **25**(16), 6287–6296.
33 S. Fajal, S. Dutta and S. K. Ghosh, Porous organic polymers (POPs) for environmental remediation, *Mater. Horiz.*, 2023, **10**(10), 4083–4138.
34 Q. Sun, B. Aguila, Y. Song and S. Ma, Tailored porous organic polymers for task-specific water purification, *Acc. Chem. Res.*, 2020, **53**(4), 812–821.
35 S. Jiao, L. Deng, X. Zhang, Y. Zhang, K. Liu, S. Li, L. Wang and D. Ma, Evaluation of an ionic porous organic polymer

for water remediation, *ACS Appl. Mater. Interfaces*, 2021, **13**(33), 39404–39413.

36 W. Chen, P. Chen, G. Zhang, G. Xing, Y. Feng, Y. W. Yang and L. Chen, Macrocycle-derived hierarchical porous organic polymers: synthesis and applications, *Chem. Soc. Rev.*, 2021, **50**(20), 11684–11714.

37 B. Aguila, Q. Sun, J. A. Perman, L. D. Earl, C. W. Abney, R. Elzein, R. Schlaf and S. Ma, Efficient mercury capture using functionalized porous organic polymer, *Adv. Mater.*, 2017, **29**(31), 1700665.

38 X. Feng, X. Ding and D. Jiang, Covalent organic frameworks, *Chem. Soc. Rev.*, 2012, **41**(18), 6010–6022.

39 S. Y. Ding and W. Wang, Covalent organic frameworks (COFs): from design to applications, *Chem. Soc. Rev.*, 2013, **42**(2), 548–568.

40 P. J. Waller, F. Gándara and O. M. Yaghi, Chemistry of covalent organic frameworks, *Acc. Chem. Res.*, 2015, **48**(12), 3053–3063.

41 N. Huang, P. Wang and D. Jiang, Covalent organic frameworks: a materials platform for structural and functional designs, *Nat. Rev. Mater.*, 2016, **1**(10), 1–19.

42 A. P. Cote, A. I. Benin, N. W. Ockwig, M. O'Keeffe, A. J. Matzger and O. M. Yaghi, Porous, crystalline, covalent organic frameworks, *Science*, 2005, **310**(5751), 1166–1170.